Korean Membrane Journal
Vol. 3, No. 1, December, 2001, 59-68

Separation of Colloidal Particles by Osmotic Sink Field Flow Fractionation Using UF Hollow Fiber Membranes

Se-Jong Shin, Byoung-Ryul Min†, Jin-Won Park, Ik-Sung Ahn, Kang-Taek Lee, and Jae-Hoon Lee[1]

Dept. of Chem. Eng., Yonsei Univ., Seoul 120-749, Korea
[1]Korea Energy Management Corporation, Gyunggi-Do 449-994, Korea
(Received December 2, 2001, Accepted December 22, 2001)

Abstract : Unlike existent field flow fractionation, new method, osmotic sink field flow fractionation is introduced and used ultrafiltration hollow fiber membranes as separation channel. This hollow fiber osmotic sink field flow fractionation is called HF-OSFFF. A theory that describes the retention, relaxation, resolution, plate number for the system, has been developed and experimentally verified by separation model of polystyrene latex beads. At external field, it is measured that radial flow rates change according to various concentrations of PEG solutions. Concentration of PEG solution vs. radial flow rate is a linear relation. For diameter distribution of unknown polymer sample, HF-OSFFF compared with the commercial capillary hydrodynamic flow fractionation (CHDF).

Keywords : *hollow fiber membrane, osmotic sink field flow fractionation, plate number, resolution, retention time, relaxation time.*

1. Introduction

In 1966 a new concept for the separation of macromolecules and particles was introduced by Giddings [1]. Separation techniques based on this concept are called field flow fractionation (FFF). FFF was slowly developed after its introduction in 1966. Requirements of the high resolution of FFF instrumentation and the intrinsic difficulties of the treatment of the macromolecular and colloidal materials obstructed the initial development of FFF. Recently, however, a lot of research groups started to have strong interest in FFF. For example, Kirkland and Yau at the DuPont Company has been developed the sedimentation FFF, one of the subtechniques of FFF [2,3]; this appears to be a precusor for the industrial application of FFF. Presently, it is expected that the potential for the application of FFF is enormous. It seems that FFF can apply to almost all types of separation of soluble and suspended macromolecular or colloidal materials. The solvent and suspended medium can be aqueous or organic. The particles may be charged, uncharged, random coils, or globular; they may originate from a consequence of industrial, biological, environmental, or geological activities.

In FFF, some kinds of externally adjusted fields have to be applied for the fractionation of the suspended particles in the channel [4]. The application of an external force field to a solution causes a migration of its constituents toward the separation channel wall. Close to the separation

†Author for all correspondences
(e-mail : minbr345@yonsei.ac.kr)

channel wall, the sample cloud will develop an exponential concentration distribution and form a zone, which has a specific average thickness. The thickness of the zone depends on the magnitude of the force field and the physical and chemical properties of the sample. If the liquid in the channel at this point is under laminar flow conditions, a parabolic flow profile will develop. An individual particle will move forward with a velocity corresponding to its mean lateral position in a parabolic flow profile. The velocity of the sample zone can be determined by its average thickness as introduced by Giddings [1].

Janca classified FFF types according to the external field applied [4]. They are the thermal FFF by thermal gradients, the sedimentation FFF by centrifugal forces, the electrical FFF by electrical forces, the flow FFF by transverse or lateral flows, and the pressure FFF by transverse pressure gradients. The flow FFF(FFFF), which utilizes a transverse secondary flow through a semi-permeable membrane as the external field, is the most popular FFF technique. FFFF has been studied intensively for virus samples, proteins, silica sols, and synthetic polymers of lipophilic and hydrophilic [5,6,7,8,9]. Recently Wahlund et al. and Giddings et al. made significant technical improvements in FFFF [10-12]. They reported the shorter elution times and the better resolutions.

Osmotic sink FFF(OSFFF) is a new subtechnique and is related to FFFF. In both FFFF and OSFFF, a cross flow or a radial flow represents the lateral field as the external field applied. The difference between FFFF and OSFFF is that in FFFF, the flow field is applied across the channel by a separate pump, while in OSFFF, it is created by an osmotic pressure over the semi-permeable membrane.

In this work, a new approach using a cylindrical hollow fiber for OSFFF was studied. Generally, the simple operation and the independent control of the elution and radial flows are mentioned as the advantages of a cylindrical hollow fiber FFF. Also, the cylindrical channel automatically tends to maintain its cylindrical cross section when pressurized. A circular hollow fiber configuration for OSFFF has been used in this study and it appeared that this configuration has many advantages such as better mechanical properties and easier connections to liquid chromatographic equipment. These permit the technically simple construction of the separation channel with the defined geometry, as a pressurized flexible tube automatically tends to form a perfect cylindrical cross-section. In addition, flow rates can be more precisely controlled. The channel is, in most cases, a membrane made of polysulfone or cellulose-based materials with a homogeneously porous surface, the skin-like surface. For stability this smooth surface is supported by the more rigid and coarse membrane structure. Typical molecular weight cutoff of the membranes in FFFF and OSFFF is between 5,000 and 100,000.

Jnsson and Carlshaf, recently, reported their theoretical and experimental results using a semi-permeable hollow fiber as the separation channel for FFFF [13-15]. The theoretical basis of the hollow-fiber OSFFF is similar to that of the hollow-fiber FFFF. Therefore, it is possible to calculate the diffusion coefficient and the Stokes diameter of the particles for uncharacterized molecules and colloidal particles from retention parameters measured. This work aimed at analyzing the mixture of standard polymer samples of polystyrene latex beads to calculate retention times, plate numbers, resolutions, etc. Also, the diameter distribution measured using HF-OSFFF was compared with that measured using CHDF.

Theoretical Background

The theoretical background used in this work is introduced below. Kedem-Katchalsky developed the following equation to see the effect of the osmotic sink on the radial flow rate [16]. Linear average velocity (J_v) on the radial flow is given by:

$$J_v = L(\triangle P - \sigma \triangle \Pi) \quad (1)$$

The relationship between the flow velocities and the volumetric pump flow rates can be expressed by Equations (2) and (3) [17,18].

$$V_{in}^{\&} = \bar{u}_z(0)\pi\gamma_{HF}^2 \tag{2}$$

$$V_{rad}^{\&} = 2\pi\gamma_{HF}\int_0^L u_r(r_{HF}, z)dz = \frac{2\pi\gamma_{HF}u_r(R,0)}{\alpha}\cdot(1-\exp(-\alpha\cdot L_{HF})) \tag{3}$$

The principal parameter in the theory is the Peclet number (Pe) which is defined as

$$Pe \equiv u_{r(\gamma_{HF}, z)}\frac{r_{HF}}{D} \tag{4}$$

Pe is proportional to the radial flow rate and inversely proportional to the diffusion coefficient. It describes the normalized mean distance between the particles and the fiber wall relative to the fiber radius (r_{HF}). Assuming that a particle of radius r_s just touches the wall, the distance (r) from the tube center can be given by:

$$r = r_{HF} - r_s \tag{5}$$

$$x = 1 - r_s/r_{HF} \tag{6}$$

By expressing the travel velocity of the particle, the following equation can be obtained.

$$\frac{r_s}{r_{HF}} = 1-\left(1-\frac{2}{Pe}\right)^{1/2} \approx \frac{l}{Pe} \tag{7}$$

The mean distance () of the particles from the wall can be derived from Equation 7 and be represented by:

$$l \approx \frac{r_{HF}}{Pe}\cdot \tag{8}$$

For large Pe numbers (Pe > 50), the retention time can be given by:

$$t_R = \frac{(L_{HF}-\zeta)}{\bar{u}_z}\cdot\frac{Pe}{4}\cdot \tag{9}$$

Equation (9) can be derived mathematically by assuming that Pe is a constant [19]. However, from the definition of Pe, it is obvious that in a real case, Pe will vary along the fiber. This question is addressed below.

Doshi et al. [20] have derived a Gaussian function to describe the peak shape. The following equation describing the retention time in the hollow fiber FFFF system is obtained through the rearrangement of the function.

$$dt_R = \frac{Pe(z)}{4\bar{u}_z(z)}\left[1-\frac{4}{Pe(z)}+\frac{72}{Pe^2(z)}-\Lambda\right]^{-1}dz \tag{10}$$

In Equation (10), $Pe(z)$ and vary along the fiber. For large Pe numbers, the integration of Equation (10) gives

$$t_R = \frac{R^2}{8D}\ln(\bar{u}_z(\zeta)/\bar{u}_z(L)) \tag{11}$$

As the axial flow rate increased, the measured retention time greatly deviated from the theoretical values calculated by Equation (11). The expected plate number, N, can be calculated in a similar way. For large Pe numbers the following equations can be derived for the theoretical plate number.

$$D = \frac{kT}{6\pi\mu r_s} \tag{12}$$

$$t_R = \frac{3\pi\mu r_s r_{HF}^2}{4kT}\ln(\bar{u}_z(\zeta)/\bar{u}_z(L_{HF})) \tag{13}$$

$$N = \frac{\bar{u}_r^2}{4D}t_R \tag{14}$$

These equations can be used to predict the retention time and the efficiency of HF-OSFFF developed in this study as an OSFFF system. Also, they were used in this work to calculate theoretical values of retention times and plate numbers. Meanwhile, the sample concentration and the homogeneity of the pore distribution in the fiber wall influence on the practically achievable plate number. Therefore, the experimental plate number in this work was calculated by

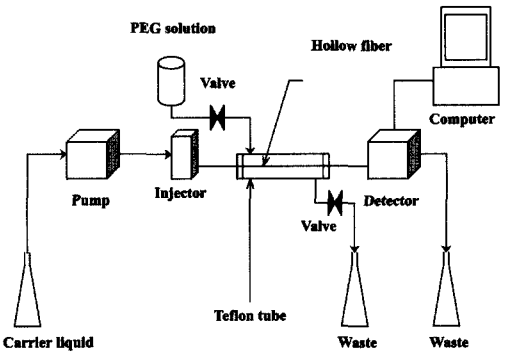

Fig. 1. The schematic diagram of HF-OSFFF.

$$N = \frac{t_R^2}{\tau^2} = 1.38629 \frac{t_R^2}{\tau_{1/2}^2} \quad (15)$$

where is half height of peak [21].

Materials and Methods

A schematic diagram of the HF-OSFFF system used in this work is presented in Figure 1. The main equipment used was standard HPLC (High Performance Liquid Chromatography) devices from UPCHURCH located at Oak Harbor, USA. The FFF channels were 25 cm-long polysulfone (PSf) hollow fibers (HF) from Sunkyong Industries (Suwon, Korea). The inner diameter of fibers (d_{HF}) was 0.8 mm. The inner wall of the membranes used have a skinlike surface supported by an open-celled structure. It provides a smooth inner surface, high mechanical strength, and high permeability. The molecular weight cutoff is 10,000. The fiber was encapsulated in a diameter of 1/4 〃 teflon tube column and was equipped with tee unions (JACO, USA). To attach the fiber to the endpieces and to connect it to the flow streams, the standard high pressure capillary tube fittings (Swagelok, USA) were used. The column was connected to the injector and the detector. A mobile phase was delivered by a standard HPLC pump (Model 930, YoungLin, Korea) capable of maintaining constant flow rates from 0.001 to 20.0 mL/min. The radial flow was generated by the osmotic pressure using a polyethylene glycol (PEG) solution, which used to extract a liquid through the fiber walls. The radial flow rate was measured to the difference between $V_{in}^{\&}$ and $V_{out}^{\&}$. PEG used in this study was MWCO 35,000 (Fluka, Swiss). The liguid was delivered to the outer column compartment and was thrown away. The annular stream of the PEG solution was created by gravity and the stream was controlled by a metering valve (NUPRO, USA). A sample was introduced into the system by using a pneumatically controlled injection valve (Model 7725I, Rheodyne, Cotati, CA, USA) with internal loops.

The fractograms showing a detector signal as a function of an elution time were obtained with an UV detector at 254 nm (Model 720, YoungLin, Korea) and were recorded by an autochro data module (YoungLin, Korea). As shown in Figure 1, the outlet tube from the detector is very long. It is necessary because during the relaxation phase, the liquid could be drawn backward to the fiber.

Polystyrene latex beads of diameters of 50, 96, 204, and 304 nm (Duke Scientific Corp., California, USA) was used in this study. The particles were diluted in the elution media contented 0.04% solid and the solution was sonicated about 1 hour before use to avoid particle aggregation. The sonication had to be repeated after about 4 hours use. The carrier solutions used were the distilled water included the 0.1% FL-70 surfactant solution and the 0.02% sodium azide. These eluents were also used as carriers in the elutions and they did not cause the noticeable degradation of the hollow fiber after long time contant. The PEG solutions for the osmotic pressure were prepared with the different molar concentrations of the distilled water at the same concentration of 0.02% sodium azide. All chemicals used in this work were of the HPLC grade and the water was purified using a UHQ/RO Type LC 102 (ELGA, England).

Results and Discussion

The relaxation process has been optimized for

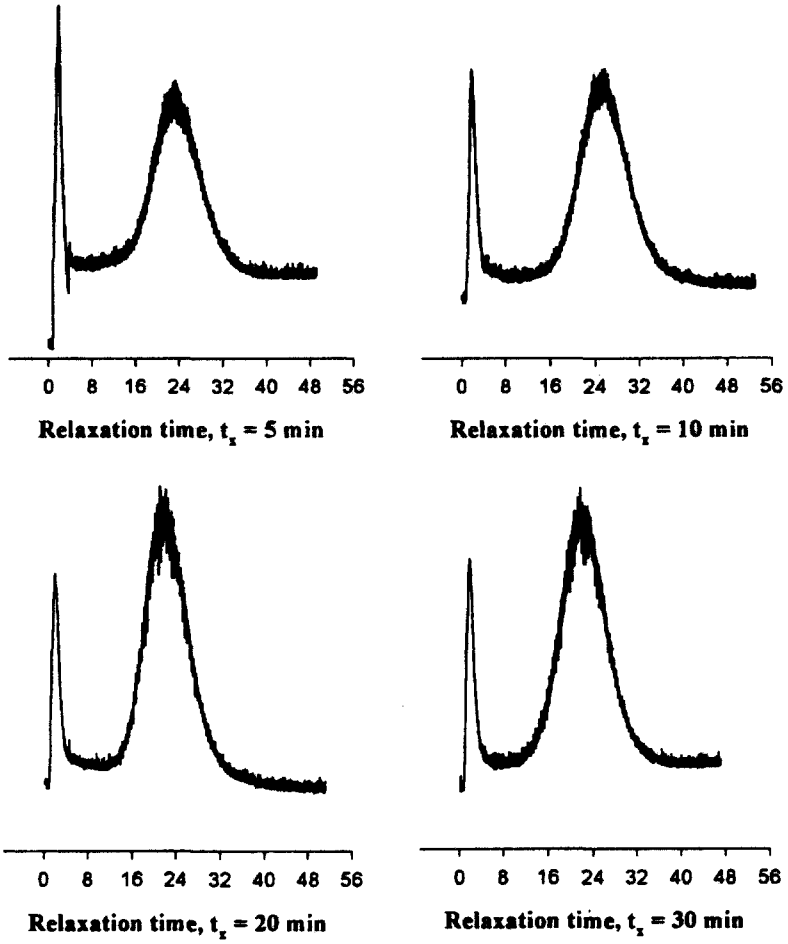

Fig. 2. Fractograms showing a relaxation effect of a 96 nm PSL for different relaxation time tx, and successive elution : $V^{\&}_{in}$ = 0.31 mL/min, $V^{\&}_{rad}$ = 0.06 mL/min.

the system with latex beads (96 mm). Figure 2 shows the fractograms as a function of the relaxation times (t_x). The PSf fiber (MWCO, 10,000) was used and the radial flow rate ($V^{\&}_{rad}$) was 0.06 mL/min in all runs. The inlet flow rate ($V^{\&}_{in}$) was increased from 0.005 mL/min to 0.31 mL/min. The fraction, already located near the fiber wall, retards and elutes as a broad peak. As the relaxation time is successively increased, the void peak is decreased for the retarded sample peak. At the relaxation time of 20 min, the intensity of the void peak was almost constant. It indicated that the radial concentration distribution reached its equilibriun state and the same is retarded in the fiber as expected. The relaxation time calculated was 21 min. But, for the longer relaxation time, more than 30 min, the void peak was increased due to the axial diffusion of the sample.

Figure 3 presents a comparison between the experimental and the theoretical retention times as a function of the radial flow rate. In that case the FL-70 0.1% solution was used as the carrier solution. As the radial flow rate increased, the retention time of the large particle sample (PS) of304 nm greatly deviated from the theoretocal values. The difference resulted from the steric effect of the large particles with the increased field strength. This occurs for the high field

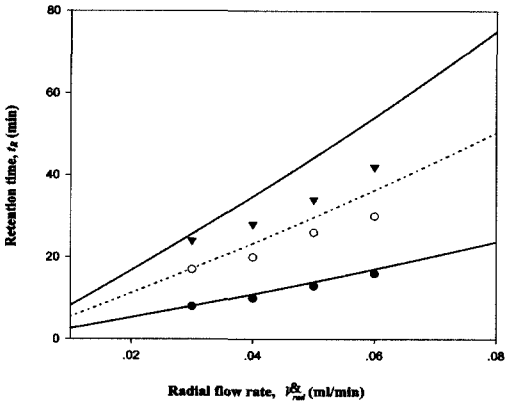

Fig. 3. Experimental (points) and theoretically calculated values (curves) of t_R versus $\dot{V}_{rad}$: at = $\dot{V}_{in}$ 0.31 mL/min, ●: PS 96 nm ○: PS 204 nm ▼: PS 304 nm.

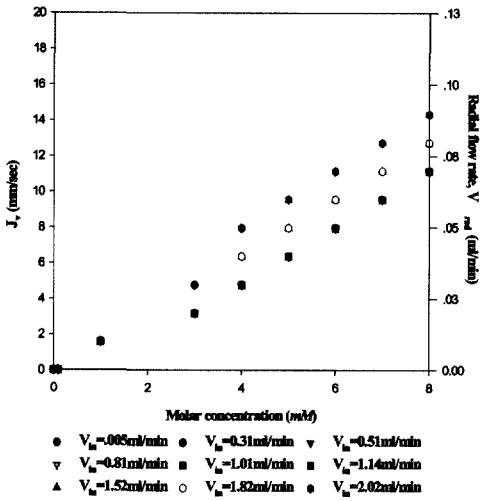

Fig. 4. Effect of concentration variation on radial flow rate.

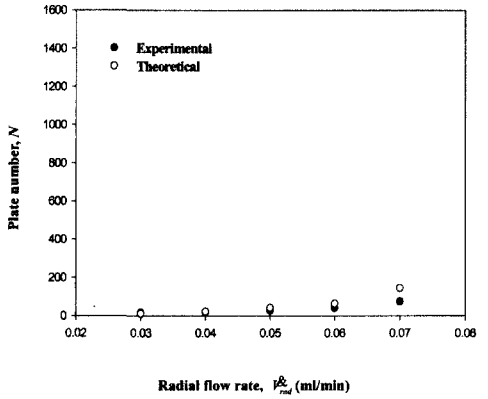

Fig. 5. Comparison with the experimental plate number and the theoretical plate number versus $V^{\&}_{rad}$ at $V^{\&}_{in}$ = 0.31 mL/min, PS 96 nm (4 mg/mL).

strength applied and in that case particles can be rolling on the wall. Because of that, the larger particles occupy more space in the faster moving streamlines, causing the decrease of the retention time. A detergent was used to prevent the aggregation of particles; the type of the surfactant might have an influence on the retention time because it could adhere to the surfaces and alter the properties of the particles.

According to variant molar concentration, radial flow rate is changed. Linear average velocity (J_v) on radial flow is obtained by Kedem-Katchalsky equation (1). is obtained by Vant' Hoff equation. J_v and radial flow rate ($V^{\&}_{rad}$) versus molar concentration are compared. This relation is linear and not effected nearly by axial flow rate ($V^{\&}_{in}$). This radial flow rate changes according to osmotic pressure at Figure 4.

The efficiency of the HF-OSFFF system was determined using the experimental plate number (N). It is generally lower than the theoretical efficiency calculated by Equation (12). The sample concentration and the homogeneity of the pore distribution in the fiber wall influnce on the practical plate number. The plate numbers experimentally obtained in this study are shown in Figure 5, 6, and 7. PS of 96 nm, PS of 204 nm, and PS of 304 nm were used in the figures, respectively. In those figures, the experimental plate numbers are considerably lower than the theoretical plate ones. The difference increases as the radial flow rate increases. There may be several reasons for the discrepancy. One of them, already mentioned above, is the possibility of the onset of the steric effect. Others include the axial diffusion of the sample particles, the polydispersity of the particles, the finite injection volume, and the inhomogeneity of the fiber porosity. Equation (14) does not consider theses

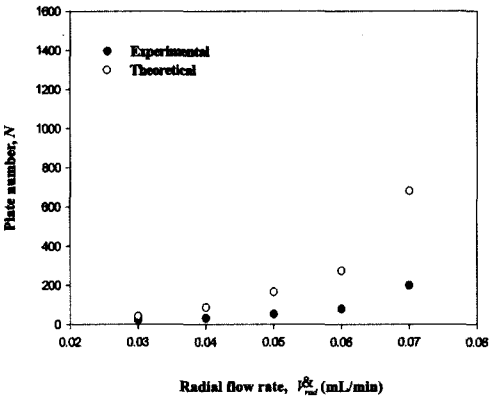

Fig. 6. Comparison with the experimental plate number and the theoretical plate number versus $V^{\&}_{rad}$ at $V^{\&}_{in}$ = 0.31 mL/min, PS 204 nm (4 mg/mL).

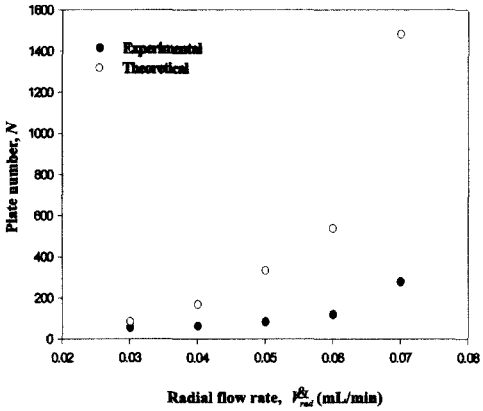

Fig. 7. Comparison with the experimental plate number and the theoretical plate number versus $V^{\&}_{rad}$ at $V^{\&}_{in}$ = 0.31 mL/min, PS 304 nm (4 mg/mL).

pratical facts because it is derived theoretically. It seems that those facts cause the difference. Probably the main reason is the inhomogeneity of the fiber porosity. These fibers are produced for the purpose of industrial-scale filtration and are relatively low-priced. If the permeability of the fiber varies slightly at different places, it will not have adverse effects for industrial uses. Also, it will not appreciably influence on the retention time because local high radial flows, responsible for the increase of the local retention time, inhigh permeability regions are balanced by low

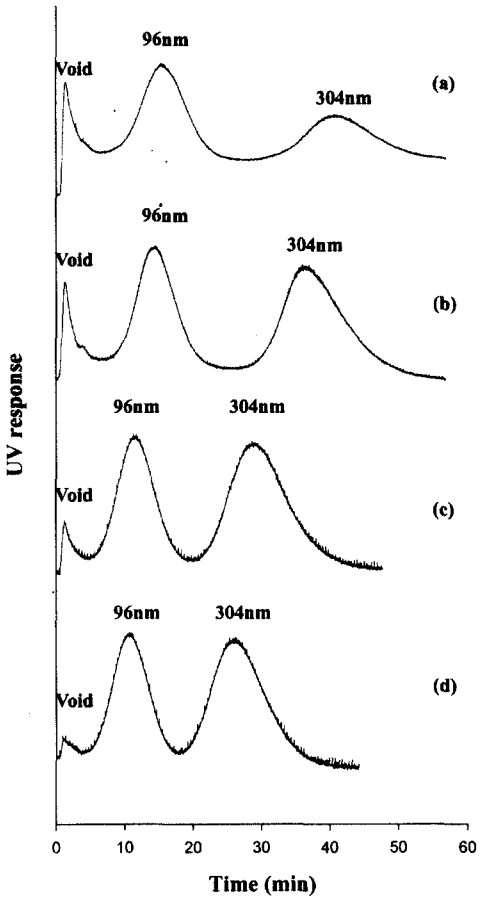

Fig. 8. Elution profiles of polystyrenes (96+304 nm) by varying radial flow rate, at tx = 30 min, $V^{\&}_{in}$ = 0.31 mL/min : (a) $V^{\&}_{rad}$ = 0.06 mL/min, (b) 0.05 mL/min, (c) 0.04 mL/min, (d) 0.03 mL/min.

radial flows in other regions. Therefore, the observed mean retention time can be determined by the mean radial flow. That, however, can increase the band broadening. Some fibers have a distinct groove along their outer surfaces and these fibers were not suitable for the purposes of this work. A careful selection of individual fibers through considering the uniformity of the porosity, the degree of the elasticity, and the hollow fiber manufacturing process maybe provide an improved performance of the HF-OSFFF technique.

Figure 8 and 9 show the example of the separation of the polystyrene latex beads using

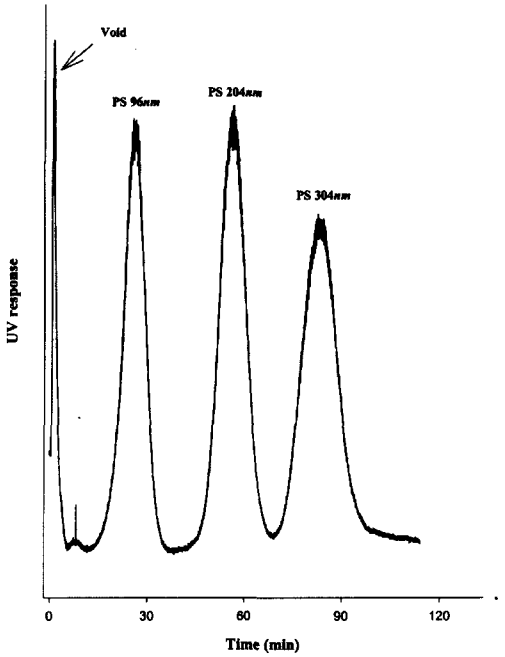

Fig. 9. The separation of three components (96 + 204 + 304 nm) : t_x = 30 min, $V^{\&}_{in}$ = 0.31 mL/min, $V^{\&}_{rad}$ = 0.07 mL/min.

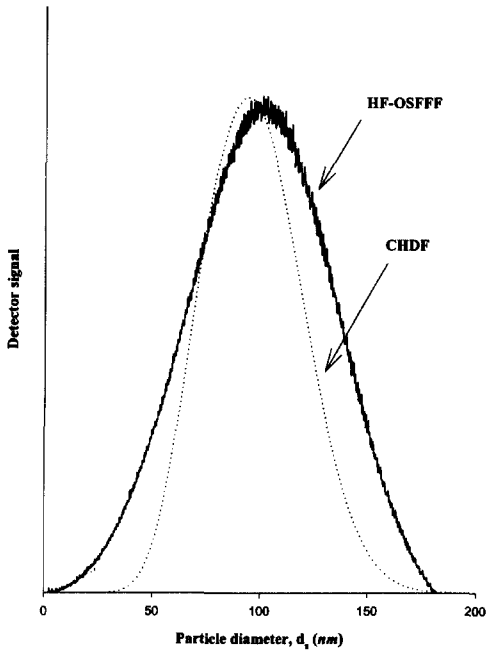

Fig. 10. Comparison with the diameter distribution of HF-OSFFF and CHDF. From CHDF: PSt/SAA, Dn=98.4 nm, St.Dev. =23.1 nm From HF-OSFFF: d_s=100.8 nm.

the PSf fiber. This analysis was performed by an UV detector. Figure 8 presents the change of the retention time as a function of the radial flow rates for the separation of the two components. As the radial flow rate decreases, the retention time also decreases. For the fast analysis of the mixture, the weak field strength and the quick axial flow rate were required. Figure 9 shows the separation of the three components (96, 204, and 304 nm). It was separated completely at the operating conditions of $V^{\&}_{in}$=0.31 mL/min, $V^{\&}_{rad}$ =0.07 mL/min, and t_x=30 min. The conditions show that the ratio of the axial flow rate to the radial flow rate is small and the particles are affected by the high field strength. As the result, the separation of the mixture containing more components was done under the low ratio of the axial flow rate to the radial flow rate and the high field strength.

Generally, large particles elute faster than small ones and separation is performed in order of the particle size under the laminar flow in the narrow bore capillaries. This technique is called CHDF. The size exclusion of the particles from the slow moving streamlines and the colloidal and inertial forces acting on the particles cause the separation. It is known that this analysis is based on a fundamental model for the convected Brownian motion of colloidal particles in a capillary tube. In this study, the polymer sample of PSt/SAA was analyzed by CHDF and HF-OSFFF. Figure 10 shows the diameter distributions measured by CHDF and by HF-OSFFF. The distribution by HF-OSFFF is more broad because of the peak broadening at the intensive field strength. The important parameter that affects the elution behavior is the sample load. Too high concentration of the particles in the sample zone can lead to increased particle-particle interactions; therefore, the particles cannot be approximated any more as the non-interacting point particles in the theory. The overloading causes the deviation

from the ideal behavior. The sample zone can reach the overcrowded state without the sample overloading for inappropriate separation conditions. The characteristics of the sample were determined using the distribution by CHDF. They were D_n=98.4 nm, D_w=111.2 nm, and St.Dev.=23.1. For the distribution by HF-OSFFF, the maximum signal was detected at d_s=100.8 nm. That was very close to the maximun signal of the distribution by CHDF.

It is necessary to know the effective diameter of the hollow fiber membrane ($d_{HF,eff}$) to calculate the precise plate number, the retention time, the relaxation time, etc. The $d_{HF,eff}$ was measured by the optical microscope of the Nikon SMZ-2T model and was 0.8 nm.

Conclusions

Osmotic sink FFF (OSFFF), one of the new FFF subtechniques was studied and the HF-OSFFF system based on OSFFF was developed in this work. The HF-OSFFF system used hollow fiber membranes.

The radial flow rates were measured as a function of the molar concentrations of the PEG solutions. This measurement provided the accurate ratio of the axial flow rate to the radial flow rate. The operating conditions for the separation of the mixture of the spherical polymer standard samples of the polystyrene latex beads were determined. As the radial flow rate decreases, the retention time also reduces. The operating conditions of the separation of the three components were =0.31 mL/min, =0.07 mL/min, and =30 min. It was found that the separation of the mixture of the more particles could be possible under the low ratio of the axial flow rate to the radial flow rate and the high field strength.

The number of the practical plate was obtained using the fractograms of the mixture and the effective diameter of HF at different operating conditions. The number of the experimental plate is quite lower than that of the theoretical plate. It seemed that this difference resulted from the steric effect, the axial diffusion, the polydispersity of the sample, and the inhomogeniety of the porosity of the membrane.

The particle diameter distributions of PSf/SAA were measured using CHDF and HF-OSFFF. The comparison between the distributions showed the possibility of HF-OSFFF as a commercial analytical technique.

Acknowledgement

This work was partially supported by grant NO. (R01-2001-00420) from the Korea Science Engineering Foundation.

Nomenclatures

c	total concentration (mol/cm^3)
d_s	particle diameter (nm)
d_{HF}	hollow fiber diameter (nm)
D	diffusivity (cm^2/min)
H	plate height
L_{HF}	fiber length (cm)
Pe	Peclect number
r	radial coordinate
r_{HF}	fiber radius (m)
t_R	retention time (min)
t_x	relaxation time (min)
u_r	radial flow velocity (cm/min)
u_w	velocity at the wall (cm/min)
u_z	axial flow velocity (cm/min)
v_r	radial particle velocity (cm/min)
v_z	axial particle velocity (cm/min)
$V^{\&}_{in}$	inlet flow rate (mL/min)
$V^{\&}_{out}$	outlet flow rate (mL/min)
$V^{\&}_{rad}$	radial flow rate (mL/min)
z	axial coordinate
β	permeability (cm^3/cm^{2}atm)
η	viscosity (g/cm s)
σ	standard deviation (min)
ξ	relaxation point (cm)

References

1. J. C. Giddings. *Sep. Sci.* 1, 123 (1966).
2. J. J. Kirkland, C. H. Dilks, Jr., and W. W. Yau. *J. Chromatogr.*, **255**, 255 (1983).
3. J. J. Kirkland, S. W. Rementer, and W. W. Yau. *Anal. Chem.*, **53**, 1730 (1981).
4. J. Janca, Field-Flow Fractionation, Marcel Dekker, Inc., New York (1987).
5. J. C. Giddings, F. J. Yang, and M. N. Myers, *J. Virol.*, **21**, 131 (1977).
6. J. C. Giddings, F. J. Yang, and M. N. Myers, *Anal. Biochem.*, **81**, 395 (1977).
7. J. C. Giddings, G. C. Lin, and M. N. Myers, *J. Colloid interface Sci.*, **65**, 67 (1978).
8. S. L. Brimhall, M. N Myers, K. D. Caldwell, and J. C. Giddings, *J. Polym. Sci., Polym. Lett. Ed.* **22**, 339 (1984).
9. J. C. Giddings, G. C.Lin, and M. N. Myers, *J. Liq. Chromatogr.*, **1**, 1 (1976).
10. K. G. Wahlund, H. S. Winegartner, K. D. Caldwell, and J. C. Giddings, *Anal Chem.* **58**, 573 (1986).
11. K. G. Wahlund and J. C. Giddings, *Anal. Chem.* **59**, 1332 (1987).
12. J. C. Giddings, C. Xiurong, K. G. Wahlund, and M. N. Myers, *Anal. Chem.* **59**, 1957 (1987).
13. A. Carlshaf and J. A. Jnsson, *J. Chromatogr.*, **461**, 89 (1989).
14. A. Carlshaf and J. A. Jnsson, *J. Microcol. Sep.*, **3**, 411 (1991).
15. J. A. Jnsson and A. Carlshaf, *Anal. Chem.*, **61**, 11 (1989).
16. M. Mulder, "Basic Principles of Membrane Technology," Kluwer Academic Publishers, Inc. (1991).
17. A. A. Kozinski, F. P. Schmidt, and E. N. Lightfoot, *Ind. Eng. Chem.* **48**, 1126 (1976).
18. R. B. Bird, W. E. Stewart, E. N. Lightfoot, "Transport Phenomena," John Wiley & Sons, Inc. (1960).
19. H. L. Lee, J. F. G. Reis, J. Dohner, and E. N. Lightfoot, *J. AIChE.*, **20**, 776 (1974).
20. M. R. Doshi and W. N. Gill, *Chem. Eng. Sci.*, **34**, 725 (1979).
21. J. C. Giddings, "Unified Separation Science," John Wiley & Sons, Inc. (1991).